

Cosmo++: An Object-Oriented C++ Library for Cosmology

Grigor Aslanyan

Department of Physics, University of Auckland, Private Bag 92019, Auckland, New Zealand

Abstract

This paper introduces a new publicly available numerical library for cosmology, Cosmo++. The library has been designed using object-oriented programming techniques, and fully implemented in C++. Cosmo++ introduces a unified interface for using most of the frequently used numerical methods in cosmology. Most of the features are implemented in Cosmo++ itself, while a part of the functionality is implemented by linking to other publicly available libraries. The most important features of the library are Cosmic Microwave Background anisotropies power spectrum and transfer function calculations, likelihood calculations, parameter space sampling tools, sky map simulations, and mask apodization. Cosmo++ also includes a few mathematical tools that are frequently used in numerical research in cosmology and beyond. A few simple examples are included in Cosmo++ to help the user understand the key features. The library has been fully tested, and we describe some of the important tests in this paper. Cosmo++ is publicly available at <https://github.com/aslanyan/cosmopp>.

Keywords: Cosmology, Cosmic Microwave Background, C++

1. Introduction

Numerical methods are an indispensable part of modern research in cosmology, from theoretical studies to experimental data analysis. In this paper we introduce a new numerical library for cosmology in C++, Cosmo++. We use object-oriented programming to separate different parts of the library into different classes, resulting in an intuitive and easy-to-understand user interface.

Numerous excellent numerical libraries and packages have been developed and rigorously tested in the past 2 decades, including HEALPix [1], CAMB [2], CLASS [3, 4], WMAP likelihood code [5, 6, 7], Planck likelihood code [8], CosmoMC [9]. Cosmo++ is not intended to replace any of the existing packages, but rather complement them with a clear interface and some additional

Email address: g.aslanyan@auckland.ac.nz (Grigor Aslanyan)

tools that are frequently used in cosmological research. The main features of the library are likelihood calculation for Cosmic Microwave Background (CMB) data, parameter space sampling tools, an interface to the publicly available Boltzmann code CLASS [3, 4] for CMB power spectrum and transfer function calculations, a mask apodization tool, sky simulation tools, and a few mathematical utilities frequently used in numerical research in physics. The library is made of many independent modules (classes in C++), which can be used on their own or easily combined together. This allows the user to include their own code if desired, without any need to modify the existing code. They can implement their own version of any of the modules and combine them with the rest of the library. This is accomplished through the usage of inheritance, polymorphism, and template parameters. For example, the primordial power spectrum is treated as just a regular real function. To implement a new form of the primordial power spectrum, the user needs to simply inherit a new class from the given abstract class of a real function, and then pass an object of their new class into the functions of the library.

Since there are a few publicly available excellent Boltzmann solvers [2, 3, 4], Cosmo++ does not include a new one. It rather includes a clear interface for a Boltzmann solver, which is linked to CLASS. The Boltzmann solver is included as a completely independent module, allowing the user to easily switch to a different one.

Likelihood calculation tools are included both for large and small scales. One important feature of Cosmo++ is temperature and polarization likelihood calculation for off-diagonal covariance matrices in harmonic space. The standard Λ CDM model assumes statistical isotropy of the universe, implying diagonal covariance matrices in harmonic space. However, some proposed extensions of Λ CDM, such as a non-trivial topology of the universe [10, 11] and anisotropic models of inflation [12, 13], break the statistical isotropy of the universe. In light of the large-scale anomalies detected in the CMB data [14], anisotropic models of the universe need to be rigorously tested. The large-scale likelihood calculators included in Cosmo++ are indispensable tools for such tests.

Two different parameter space samplers are included in Cosmo++, a Metropolis-Hastings sampler [15] and an interface to the publicly available MultiNest sampler [16, 17, 18]. This allows the user to easily switch between the samplers or even implement and include their own sampler.

The library is fully documented using Doxygen [19]. In this paper we describe the general functionality of the library, and the specifics of implementation.

This paper is organized as follows. Sections 2 - 6 describe the main functionality of the library. In Section 7 we describe some mathematical tools that are frequently used in cosmology and other areas of physics. We introduce a few examples in Section 8, showing the usage of the main features of the library in only a few lines of code. We describe some of the most important tests performed in Section 9, and we summarize in Section 10. Our notation and units are described in Appendix A.

2. Cosmological Parameters and Power Spectra

2.1. Cosmological Parameters

The cosmological parameters can be described by inheriting a class from the abstract class *CosmologicalParams* (defined in `cosmological_params.hpp`) and implementing all of the virtual functions. The virtual functions must simply return the values of different parameters. For example, the function *getOmBH2* must return the value of $\Omega_b h^2$ (see Appendix A.1 for our notation).

The class includes all of the standard Λ CDM parameters, as well as certain frequently used non-standard parameters. Instances of this class can be used to pass the cosmological parameters to other modules of the library. In particular, the class *CMB* described below takes an object of type *CosmologicalParams* as its input to calculate the CMB power spectra and transfer functions.

The primordial power spectrum is defined in *CosmologicalParams* as a general real function, as described below in Section 2.2. In addition to that, *CosmologicalParams* includes the parameters describing the primordial power spectrum in the standard case, such as A_s and n_s . These parameters contain redundant information, and are only included for completeness. The code uses the general form of the power spectrum by default, and ignores the values of the redundant parameters. However, some parts of the code, such as the class *CMB*, allow the usage of the parameters instead of the general form of the power spectrum.

Some specific examples of cosmological parameters classes are included in the file `cosmological_params.hpp`. The class *LambdaCDMParams* implements the parameters for the standard Λ CDM model. *LCDMWithTensorParams* describes the cosmological parameters for tensor fluctuations in addition to the standard Λ CDM parameters. *LCDMWithDegenerateNeutrinosParams* includes massive neutrinos of the same mass.

2.2. Primordial Power Spectrum

The primordial power spectrum is simply described as a real function $\Delta^2(k)$, both for the scalar and the tensor case (see Appendix A.4 for our notation). To implement a primordial power spectrum one needs to inherit a class from the *Math::RealFunction* class (defined in the file `function.hpp`) and implement the virtual function *evaluate*. Then instances of that class can be passed to the other modules of the library to describe the primordial power spectrum.

A few standard cases of the primordial power spectrum have been implemented in the file `power_spectrum.hpp`. The *StandardPowerSpectrum* and *StandardPowerSpectrumTensor* classes implement the standard power spectra (A.14) and (A.15), respectively.

LinearSplinePowerSpectrum and *CubicSplinePowerSpectrum* classes implement the cases when the primordial power spectrum can be written as a linear or cubic spline of a given number of knots [20, 21, 22].

2.3. CMB Power Spectra and Transfer Functions

The CMB power spectra and transfer functions can be calculated using the class *CMB* in `cmb.hpp`. The underlying code for these calculations is the publicly available code CLASS [3, 4]. Cosmo++ does not include a new Boltzmann solver, it only provides a different interface for using the functionality of CLASS. This interface makes it possible to easily link the functionality provided by CLASS with the rest of the tools of the library.

CMB has to be initialized in two stages. The function *preInitialize* is used to set the general parameters, such as the maximum value of l to be used in calculations. After this the function *initialize* can be called to set the cosmological parameters, following which the functions *getCl*, *getLensedCl*, and *getTransfer* can be called to retrieve various CMB power spectra and transfer functions. In case one needs to calculate the CMB power spectra for different values of cosmological parameters, one can call the function *initialize* multiple times after one call of *preInitialize*. The division of initialization into two stages has been done with that scenario in mind; not repeating the pre-initialization saves some computing time.

The parameter *primordialInitialize* passed to the function *preInitialize* defines if the primordial power spectrum should be initialized from the general functional form, or simply from the standard parameters A_s , n_s for the scalar case and r , n_t for the tensor case. By default, the general functional form is used for primordial power spectra, however if one is using the standard case some computing time can be saved by setting the parameter *primordialInitialize* to *false* and using the standard parameters.

The parameter *wantAll* defines if the power spectra and the transfer functions should be calculated for all values of l . By default, the calculation of the power spectra is done for only some values of l and interpolated to get the full spectrum. This speeds up the calculation by about one order of magnitude with a negligible loss in accuracy. However, if very accurate calculations of the power spectra are needed, the parameter *wantAll* needs to be set to *true*. In particular, if one needs the transfer functions by themselves, this parameter needs to be set to *true*.

3. Likelihood Calculation

Likelihood calculation is a crucial step in any parameter estimation pipeline. Cosmo++ provides three different tools for likelihood calculation, which can be used by themselves or in combination. The perturbations are assumed to be Gaussian for all three cases.

3.1. Low- l Likelihood

In the low- l range the distribution of the C_l 's cannot be well approximated by a Gaussian distribution [23]. For this reason likelihood calculation for low multipoles is done in pixel space. Cosmo++ includes pixel space likelihood calculation functionality for temperature and polarization maps.

For Gaussian perturbations the likelihood function takes the form

$$\mathcal{L}(\mathbf{m}|S)d\mathbf{m} = \frac{\exp\left[-\frac{1}{2}\mathbf{m}^t(S+N)^{-1}\mathbf{m}\right]}{(2\pi)^{3n_p/2}|S+N|^{1/2}}d\mathbf{m} \quad (1)$$

where $\mathbf{m} = (\mathbf{T}, \mathbf{Q}, \mathbf{U})$; S and N are the signal and noise covariance matrices, respectively; n_p is the number of pixels; and the symbol $|\cdot|$ stands for determinant. The rest of the notation is explained in Appendix A.2.

For low- l modes the noise in the temperature can usually be ignored, in which case it is easier to decompose the likelihood function into temperature and polarization parts [24]. We also assume no parity violation, implying $M^{TB} = 0$ and $M^{EB} = 0$. We then define

$$\tilde{E}_{lm} = E_{lm} - M_{l'm'l m}^{TE}(M_{l''m''l'm''}^{TT})^{-1}T_{l''m''} \quad (2)$$

which gives

$$\langle \tilde{E}_{lm}T_{l'm'}^* \rangle = 0, \quad (3)$$

$$\langle \tilde{E}_{lm}\tilde{E}_{l'm'}^* \rangle \equiv M_{lml'm'}^{\tilde{E}\tilde{E}} = M_{lml'm'}^{EE} - M_{l'm''l'm''}^{TE}(M_{l''m''l''m''}^{TT})^{-1}M_{l''m''l'm'}^{TE}. \quad (4)$$

Further, defining

$$\tilde{Q}(\hat{\mathbf{n}}) = \frac{1}{2} \sum_{lm} \left[\tilde{E}_{lm}(+2Y_{lm}(\hat{\mathbf{n}}) + {}_{-2}Y_{lm}(\hat{\mathbf{n}})) + iB_{lm}(+2Y_{lm}(\hat{\mathbf{n}}) - {}_{-2}Y_{lm}(\hat{\mathbf{n}})) \right], \quad (5)$$

$$\tilde{U}(\hat{\mathbf{n}}) = \frac{i}{2} \sum_{lm} \left[\tilde{E}_{lm}(+2Y_{lm}(\hat{\mathbf{n}}) - {}_{-2}Y_{lm}(\hat{\mathbf{n}})) + iB_{lm}(+2Y_{lm}(\hat{\mathbf{n}}) + {}_{-2}Y_{lm}(\hat{\mathbf{n}})) \right]. \quad (6)$$

we get $\langle \tilde{Q}(\hat{\mathbf{n}}_i)T(\hat{\mathbf{n}}_j) \rangle = 0$, $\langle \tilde{U}(\hat{\mathbf{n}}_i)T(\hat{\mathbf{n}}_j) \rangle = 0$. The likelihood function can then be decomposed into temperature and polarization parts

$$\mathcal{L}(\mathbf{m}|S)d\mathbf{m} = \frac{\exp\left[-\frac{1}{2}\tilde{\mathbf{m}}^t(\tilde{S}_P + N_P)^{-1}\tilde{\mathbf{m}}\right]}{(2\pi)^{n_p}|\tilde{S}_P + N_P|^{1/2}}d\tilde{\mathbf{m}} \frac{\exp\left[-\frac{1}{2}\mathbf{T}^tS_T^{-1}\mathbf{T}\right]}{(2\pi)^{n_p/2}|S_T|^{1/2}}d\mathbf{T} \quad (7)$$

where $\tilde{\mathbf{m}} = (\tilde{\mathbf{Q}}, \tilde{\mathbf{U}})$. The noise in the temperature has been ignored in the above equation. The noise matrix for the new \tilde{Q} and \tilde{U} variables is the same as the original Q and U noise matrix. The new signal covariance matrix can be calculated as follows

$$\begin{aligned} \langle \tilde{Q}(\hat{\mathbf{n}}_i)\tilde{Q}(\hat{\mathbf{n}}_j) \rangle &= \frac{1}{4} \sum_{lml'm'} \left[M_{lml'm'}^{\tilde{E}\tilde{E}}(+2Y_{lm}(\hat{\mathbf{n}}_i) + {}_{-2}Y_{lm}(\hat{\mathbf{n}}_i)) \right. \\ &\quad \left. (+2Y_{l'm'}^*(\hat{\mathbf{n}}_j) + {}_{-2}Y_{l'm'}^*(\hat{\mathbf{n}}_j)) - M_{lml'm'}^{BB}(+2Y_{lm}(\hat{\mathbf{n}}_i) - {}_{-2}Y_{lm}(\hat{\mathbf{n}}_i)) \right. \\ &\quad \left. (+2Y_{l'm'}^*(\hat{\mathbf{n}}_j) - {}_{-2}Y_{l'm'}^*(\hat{\mathbf{n}}_j)) \right], \end{aligned} \quad (8)$$

$$\begin{aligned}
\langle \tilde{Q}(\hat{\mathbf{n}}_i) \tilde{U}(\hat{\mathbf{n}}_j) \rangle &= \frac{i}{4} \sum_{lm'l'm'} \left[M_{lm'l'm'}^{\tilde{E}\tilde{E}} (+2Y_{lm}(\hat{\mathbf{n}}_i) + -2Y_{lm}(\hat{\mathbf{n}}_i)) \right. \\
& (+2Y_{l'm'}^*(\hat{\mathbf{n}}_j) - -2Y_{l'm'}^*(\hat{\mathbf{n}}_j)) - M_{lm'l'm'}^{BB} (+2Y_{lm}(\hat{\mathbf{n}}_i) - -2Y_{lm}(\hat{\mathbf{n}}_i)) \\
& \left. (+2Y_{l'm'}^*(\hat{\mathbf{n}}_j) + -2Y_{l'm'}^*(\hat{\mathbf{n}}_j)) \right], \tag{9}
\end{aligned}$$

$$\begin{aligned}
\langle \tilde{U}(\hat{\mathbf{n}}_i) \tilde{U}(\hat{\mathbf{n}}_j) \rangle &= -\frac{1}{4} \sum_{lm'l'm'} \left[M_{lm'l'm'}^{\tilde{E}\tilde{E}} (+2Y_{lm}(\hat{\mathbf{n}}_i) - -2Y_{lm}(\hat{\mathbf{n}}_i)) \right. \\
& (+2Y_{l'm'}^*(\hat{\mathbf{n}}_j) - -2Y_{l'm'}^*(\hat{\mathbf{n}}_j)) - M_{lm'l'm'}^{BB} (+2Y_{lm}(\hat{\mathbf{n}}_i) + -2Y_{lm}(\hat{\mathbf{n}}_i)) \\
& \left. (+2Y_{l'm'}^*(\hat{\mathbf{n}}_j) + -2Y_{l'm'}^*(\hat{\mathbf{n}}_j)) \right] \tag{10}
\end{aligned}$$

where $M_{lm'l'm'}^{\tilde{E}\tilde{E}}$ is given above by (4).

The polarization part of the likelihood can be written as follows [24]

$$\mathcal{L}(\tilde{\mathbf{m}} | \tilde{S}_P) d\tilde{\mathbf{m}} = \frac{\exp \left[-\frac{1}{2} (N_P^{-1} \tilde{\mathbf{m}})^t (N_P^{-1} \tilde{S}_P N_P^{-1} + N_P^{-1})^{-1} (N_P^{-1} \tilde{\mathbf{m}}) \right]}{(2\pi)^{n_p} |N_P^{-1} \tilde{S}_P N_P^{-1} + N_P^{-1}|^{1/2}} |N_P|^{-1} d\tilde{\mathbf{m}} \tag{11}$$

which is numerically more tractable since it contains only N_P^{-1} .

Since the calculation is done in pixel space, the formalism described above remains unchanged for a masked sky. We simply ignore the masked pixels.

3.1.1. Temperature Likelihood

The temperature part of the likelihood is implemented in the class *Likelihood* in `likelihood.hpp`. To aid the numerical regularization of matrix inversion one needs to add small noise to the signal map [25]. The class *Likelihood* therefore takes as an input the noise covariance matrix in addition to the signal covariance matrix. The noise part is usually added by hand by simulating white noise. For this reason the function *calculate* allows for input a noise map in addition to the temperature map. If the noise is already included in the temperature map, the noise map given to the function *calculate* should have 0 in all the pixels.

The covariance matrices passed to the class *Likelihood* are in pixel space. The pixel space covariance matrices (A.8) are implemented in the class *CMatrix* in `c_matrix.hpp`. The pixel space covariance matrix can be generated from the power spectrum C_l^{TT} using the function *CMatrixGenerator::clToCMatrix* in `c_matrix_generator.hpp`. The library also provides functionality for the more general case of non-diagonal covariance matrices in harmonic space, which arise if the isotropy of space is broken. The covariance matrix in harmonic space (A.9) is described by the class *WholeMatrix* in `whole_matrix.hpp`. The function *CMatrixGenerator::wholeMatrixToCMatrix* in `c_matrix_generator.hpp` can be used to convert a general harmonic space covariance matrix into pixel space, which can also perform a rotation by given Euler angles. This is a very useful feature for analyzing anisotropic models of the universe.

The class *Likelihood* takes a fiducial matrix as an input as well, which is simply added to the signal matrix. The fiducial matrix is commonly used to include

high variance monopole and dipole terms, and higher l terms not included in the signal matrix. Such a fiducial matrix can be generated using the function `CMatrixGenerator::getFiducialMatrix` in `c_matrix_generator.hpp`.

A uniform white noise matrix can be generated by `CMatrixGenerator::generateNoiseMatrix` in `c_matrix_generator.hpp`. The white noise map itself can be simulated by `Simulate::simulateWhiteNoise` in `simulate.hpp`.

The temperature likelihood calculation allows for foreground marginalization for a given template \mathbf{T}_f . A new parameter ξ is introduced into the temperature likelihood function as follows

$$\mathcal{L}_T(\mathbf{T}|C_T, \xi) = \frac{1}{(2\pi)^{n_p/2}|C_T|^{1/2}} \exp\left(-\frac{1}{2}(\mathbf{T} - \xi\mathbf{T}_f)^t C_T^{-1}(\mathbf{T} - \xi\mathbf{T}_f)\right) \quad (12)$$

where C_T denotes the total temperature covariance matrix. ξ is then marginalized over

$$\mathcal{L}_T(\mathbf{T}|C_T) = \int d\xi \mathcal{L}_T(\mathbf{T}|C_T, \xi). \quad (13)$$

The integration can be done analytically, resulting in

$$\begin{aligned} \mathcal{L}_T(\mathbf{T}|C_T) &= \frac{1}{(2\pi)^{n_p/2}|C_T|^{1/2}} \sqrt{\frac{2\pi}{\mathbf{T}_f^t C_T^{-1} \mathbf{T}_f}} \\ &\exp\left(-\frac{1}{2}\left(\mathbf{T}^t C_T^{-1} \mathbf{T} - \frac{(\mathbf{T}^t C_T^{-1} \mathbf{T}_f)^2}{\mathbf{T}_f^t C_T^{-1} \mathbf{T}_f}\right)\right). \end{aligned} \quad (14)$$

The user has the option of passing a foreground template to the constructor of `Likelihood` if she chooses to. Then (14) will be used to calculate the temperature likelihood.

`Likelihood` has the option of calculating the likelihood for many maps at the same time. Since the most time consuming part of the calculation is the inversion of the covariance matrix, a lot of computing time can be saved by initializing `Likelihood` once followed by the likelihood calculation for many maps, instead of constructing one instance of `Likelihood` for each map.

3.1.2. Polarization Likelihood

The class `LikelihoodPolarization` in `likelihood.hpp` is used to calculate the polarization part of the likelihood, according to (11). The current version does not support non-zero BB covariance matrices. The constructor takes as an input the pixel space signal covariance matrix \tilde{S}_P , the inverse noise matrix N_P^{-1} , as well as $M_{l'm'l_m}^{TE}(M_{l'm'l''m''}^{TT})^{-1}$ and T_{lm} in order to be able to calculate (2). The function `combineWholeMatrices` in `LikelihoodPolarization` can be used to construct $M_{l'm'l_m}^{TE}(M_{l'm'l''m''}^{TT})^{-1}$ and $M_{lm'l'm'}^{\tilde{E}\tilde{E}}$ from M^{TT} , M^{TE} and M^{EE} . $M_{lm'l'm'}^{\tilde{E}\tilde{E}}$ can then be converted into \tilde{S}_P using the function `CMatrixGenerator::polarizationEEWholeMatrixToCMatrix` in `c_matrix_generator.hpp`.

As for the temperature case, non-diagonal covariance matrices in harmonic space are supported. Also, likelihood calculation for many maps at once is supported.

3.2. High- l Likelihood

For high multipoles, the distribution of the C_l 's can be very well approximated by a Gaussian distribution, allowing for a much faster likelihood calculation. We follow the approach described in [26] for the implementation of high- l likelihood calculation. The current version includes high- l likelihood calculation for temperature maps only.

Before calculating the likelihood function, one needs to estimate the power spectrum \hat{C}_l^{TT} for the data. A few different approaches for this calculation have been described in the literature, including the MASTER algorithm [27], quadratic maximum likelihood (QML) estimators [28], and the XFaster algorithm [29]. The current version of Cosmo++ includes an implementation of the MASTER algorithm [27] in the class *Master* in `master.hpp`.

The first step in the power spectrum calculation is the mask coupling kernel $K_{l_1 l_2}$ using the function `calculateCouplingKernel` in the class *Master*. The mask coupling kernel is defined by [27]

$$K_{l_1 l_2} = \frac{2l_2 + 1}{4\pi} \sum_{l_3} (2l_3 + 1) W_{l_3} \begin{pmatrix} l_1 & l_2 & l_3 \\ 0 & 0 & 0 \end{pmatrix} \quad (15)$$

where $\begin{pmatrix} l_1 & l_2 & l_3 \\ 0 & 0 & 0 \end{pmatrix}$ denotes the Wigner $3-j$ symbol,

$$W_l = \frac{1}{2l + 1} \sum_{m=-l}^l |w_{lm}|^2, \quad (16)$$

and w_{lm} is the mask transformed into harmonic space. The mask coupling kernel relates the ensemble average of the masked power spectrum \tilde{C}_l to the unmasked one C_l

$$\langle \tilde{C}_{l_1} \rangle = \sum_{l_2} K_{l_1 l_2} \langle C_{l_2} \rangle. \quad (17)$$

The calculation of the mask coupling kernel is the slowest part of the whole power spectrum calculation, therefore the user is allowed to save the result in a file and use it many times for different maps. Once this is done, the result can be passed to the constructor of *Master*, then the data power spectrum can be calculated for a given map using the function `calculate`.

The high- l likelihood itself can be calculated using the class *LikelihoodHigh* in `likelihood.hpp`. This class takes as an input the output of *Master*, as well as the noise power spectrum N_l . The likelihood for a given theoretical power spectrum C_l is calculated by first calculating the cut-sky Fisher matrix [26]

$$F_{l_1 l_2} = \frac{(2l_1 + 1)K_{l_1 l_2}}{2(C_{l_1} + N_{l_1})(C_{l_2} + N_{l_2})}, \quad (18)$$

after which the likelihood function can be calculated by

$$-2 \ln \mathcal{L}(\hat{C}_l | C_l) = \sum_{l_1 l_2} (C_{l_1} - \hat{C}_{l_1}) F_{l_1 l_2} (C_{l_2} - \hat{C}_{l_2}). \quad (19)$$

The above expression assumes that $\ln \mathcal{L} = 0$ for the best fit case, i.e. the likelihood is calculated up to a fixed constant factor. Since for any practical purposes only the likelihood ratios matter (or the difference in $\ln \mathcal{L}$), the constant factor can be safely ignored.

The calculation described above assumes uniform weighting of the pixels. This is optimal in the signal dominated regime [26]. The weighting schemes that are optimal outside this regime are not supported in the current version of Cosmo++. Also, in the noise dominated regime Monte Carlo simulations might be required to accurately calibrate the Fisher matrix [26, 30]. These corrections, however, are small in the intermediate regime, and are negligible in the signal dominated regime [26]. For these reasons we do not recommend using the *LikelihoodHigh* class as it is deep into the noise dominated regime.

3.3. CMB Gibbs Sampler

Gibbs sampling has been proposed as an alternative approach to CMB power spectrum estimation and likelihood calculation [31, 32, 33]. Cosmo++ includes an implementation of the CMB Gibbs sampler in the class *CMBGibbsSampler* in `cmb_gibbs.hpp`. The implementation follows almost exactly the algorithm described in [31], so we will not go over the details here again.

The Gibbs sampler is usually used for likelihood calculation for low l values, but it can be used for l values higher than the pixel space likelihood calculation allows for. In pixel space, one can do the calculation up to $l = 30$, using reduced resolution maps with HEALPix $N_{side} = 16$, but for higher l values one needs higher resolution maps and this significantly increases the computational costs. The main reason is that one needs to invert a matrix with size equal to the number of pixels. The Gibbs Sampler, on the other hand, does not need to obtain the inverted matrix, it only needs to solve a system of linear equations, and this can be done using the preconditioned conjugate gradient algorithm [34]. Preconditioners have been proposed in the literature which allow for fast convergence; we use the preconditioner described in [31], eq. (28). This allows for fast likelihood calculation up to $l = 50$ and even higher values. A cut sky is handled by simply setting the inverse noise matrix elements to 0 for masked pixels. This approach is called the Commander implementation [31], and is used in the Planck likelihood code [8], in particular.

CMBGibbsSampler can be used to first construct the Gibbs chain and save it in a file, after which the chain can be used for very fast likelihood calculation. The Blackwell-Rao estimator [35] is used for likelihood calculation.

4. Parameter Space Sampling

Bayesian methods have become an essential part of cosmological parameter estimation in the past two decades (for a comparison of different methods see, e.g. [36]). Cosmo++ provides a general interface for parameter space sampling, which can be used for cosmological parameter estimation, in particular.

The abstract class *Math::LikelihoodFunction* in `likelihood_function.hpp` provides a simple interface for likelihood calculation from a given number of parameters. The user needs to inherit a likelihood class from *Math::LikelihoodFunction* and implement their own likelihood calculation in the function *calculate*. For example, the likelihood calculation tools described in Section 3 can be used in combination to implement a likelihood function for cosmological parameters. Section 8 includes some specific examples.

Cosmo++ includes two parameter space sampling tools, a basic Metropolis-Hastings sampler [15], and a MultiNest sampler [16, 17, 18]. The Metropolis-Hastings sampler has been implemented in Cosmo++ itself, while the MultiNest sampler uses the publicly available MultiNest code for implementation. The user has the option of not including the MultiNest code, then Cosmo++ will be compiled without the MultiNest sampler.

The Metropolis-Hastings sampler is implemented in the class *Math::MetropolisHastings* in `mcmc.hpp`, while the MultiNest scanner interface is implemented in the class *MnScanner* in `mn_scanner.hpp`. The two classes have almost identical interfaces, allowing the user to easily switch between them. The only differences in the interfaces are due to some parameters that are specific for each one of them. Both of the constructors take an instance of *Math::LikelihoodFunction* to set the likelihood function, then the parameters need to be set, including their name, range, and the prior function. After this the function *run* can be called to do the actual scan. The results are written in text files. The resulting chain files have the standard format used in cosmology codes, such as CosmoMC [9] and MultiNest [16, 17, 18]. There are publicly available standard tools that can be used to analyze the resulting chains, such as Getdist included in CosmoMC and the python package Pippi [37].

Both of the samplers allow the user to set a uniform or a Gaussian prior on the parameters. *Math::MetropolisHastings* allows the user to set an external prior function for all of the parameters in case a more general function is needed to be used or the priors of the different parameters are not independent. By default, *Math::MetropolisHastings* uses Gaussian proposal distributions, with widths that can be chosen by the user, or are set to 1/100-th of the parameter range by default. The user also has the option of setting their own proposal distribution. The parameters are varied in blocks. Each block contains one parameter by default, but the user has the option of setting their own blocks. Both of the scanners have the option of resuming from the point they stopped.

The stopping time for *Math::MetropolisHastings* is determined from the given accuracies of the parameters. Namely, the run stops when the standard deviation of the mean of all of the parameters becomes less than their accuracies. The standard deviation of the mean is calculated taking into account the auto-correlation between the elements of the chain. A maximum length of the chain must also be given to the *run* function and the run will always stop when that maximum length is reached, even if the requested accuracies are not reached. This allows the user to use other stopping criteria which can estimate the chain length required for convergence [15].

The functionality of the MultiNest scanner is described in detail in [16, 17,

18]. Our interface *MnScanner* gives two options for determining the stopping time. The user can specify whether or not they would like accurate Bayesian evidence calculation, then the code selects the recommended MultiNest parameters for each case [16].

5. Simulations

Cosmo++ provides the functionality for simulating sky maps in harmonic space. This is implemented in the class *Simulate* in `simulate.hpp`. The maps in harmonic space can be converted to pixel space using the *map2alm* function in the HEALPix C++ package.

The user has the option of simulating the sky from given C_l values or from the full covariance matrix $M_{lm'l'm'}$. The first case is similar to the HEALPix tool *synfast*, the second case is more general and allows the user to do simulations for anisotropic universes with non-diagonal covariance matrices. The non-diagonal case is implemented by switching to a basis in which the matrix becomes diagonal, then doing the simulation in the new basis, and finally switching back to the original basis. This means that the computational time and the memory requirements will increase significantly as l increases.

The class *Simulate* also provides the functionality of simulating uniform white noise maps in pixel space. This can be done using the function *simulateWhiteNoise*.

6. Other Utilities

6.1. Mask Apodization

Masks are commonly used in cosmology to separate out the reliable data points. For example, when using CMB data, one must mask out the plane of our galaxy, as well as some bright sources that cannot be reliably subtracted out from the radiation data. Sharp edges of the mask in pixel space may introduce undesirable effects when the calculation is done in harmonic space [8]. For this reason it is sometimes necessary to apodize the mask, i.e. smooth out the edges of the mask. This functionality is included in Cosmo++ through the class *MaskApodizer* in `mask_apodizer.hpp`. The input and output masks are in HEALPix format.

Two apodization types are supported: cosine and Gaussian. For the cosine apodization the 0 mask values near the edge are replaced by $\cos(\theta\pi/2\theta_{ap})$ if $\theta \leq \theta_{ap}$. Here θ denotes the angular distance from the edge, θ_{ap} is the apodization angle. In case of Gaussian apodization the 0 values are replaced by $\exp(-(3\theta)^2/2\theta_{ap}^2)$ if $\theta \leq \theta_{ap}$.

The apodization routine is implemented by first finding the pixels that are on the edge, then by scanning through all of the masked points and finding the nearest distance from the edge. The first stage is linear in the number of pixels and is relatively faster. The second stage involves $O(N_{\text{masked}}N_{\text{edge}})$ operations, where N_{masked} is the number of masked pixels, N_{edge} is the number of pixels

that lie on the edge. The computational speed of this stage depends strongly on the geometry of the mask.

6.2. Angular Momentum Dispersion Calculation

Cosmo++ includes a tool for calculating the angular momentum dispersion $\sum_m m^2 |T_{lm}(\hat{\mathbf{n}})|^2$ as a function of the direction $\hat{\mathbf{n}}$, where $T_{lm}(\hat{\mathbf{n}})$ denote the spherical harmonic coefficients in a coordinate system where the z -axis has $\hat{\mathbf{z}} \parallel \hat{\mathbf{n}}$. The main use of the angular momentum dispersion calculation is to determine the alignment of different multipoles [38, 39]. This calculation is implemented in the class *ModeDirections* in `mode_directions.hpp`. The calculation for a given direction can be done using the *calculateAngularMomentumDispersion* function. One can also find the direction which maximizes the angular momentum dispersion with the function *maximizeAngularMomentumDispersion*.

7. Mathematical Tools

Cosmo++ includes a few additional mathematical tools that are used in the implementation of the features described above. These tools are fully documented as well and can be used independently. The mathematical tools are all defined and implemented in header files, which means that the library does not need to be compiled if the user is only interested in using the mathematical tools, they simply need to include the corresponding header files in their code and compile it without the need to link it to the Cosmo++ library file.

7.1. Interpolation

Cosmo++ includes classes that provide interpolation functionality between given points. Two interpolation methods have been implemented: linear interpolation and cubic spline. Given a number of knots, the linear interpolation algorithm constructs a continuous (but not differentiable at the knots) function passing through the knots by simply connecting them by line segments. The cubic spline algorithm, on the other hand, constructs a smooth function passing through these points. The points are connected by a piecewise cubic polynomial, and the resulting curve has continuous first and second derivatives.

The linear interpolation method has been implemented in the *Math::TableFunction* class in `table_function.hpp`. This class is derived from the standard C++ class *std::map*, which gives it the full interface of *std::map*. In particular, this allows the user to define the data points using the regular interface of *std::map*. *Math::TableFunction* is also a child of the abstract class *Math::Function*, which means that an object of this type can be passed to the rest of the library wherever a one-variable function is needed. For example, an instance of *Math::TableFunction* can be used directly to represent a primordial power spectrum (see Section 2.2). The linear interpolation method has been generalized to two and three dimensions in the classes *Math::TableFunction2* and *Math::TableFunction3*, respectively. They are both in the same header file `table_function.hpp`.

The cubic spline interpolation has been implemented in the *Math::CubicSpline* class in `cubic_spline.hpp`. This class is derived from *Math::RealFunction*, allowing the user to pass an instance of *Math::CubicSpline* to the rest of the library wherever a one-variable real function is needed.¹

7.2. Conjugate Gradient Solver

The preconditioned conjugate gradient method [34] for solving a system of linear equations has been implemented in Cosmo++ in the class *Math::ConjugateGradient* in `conjugate_gradient.hpp`. Since the method can be used for potentially very big matrices, we have implemented the matrix multiplication and the preconditioning to be performed through a template type that the user needs to implement. This gives the user complete freedom in implementing the matrix multiplication. The entire matrix does not have to be stored in the memory, the user may choose to calculate each matrix element as the multiplication is performed or apply the linear operator on the vector in any other way. The simple case when the matrix and the preconditioner are known and can be set initially is implemented in the *Math::BasicCGTreats* class.

7.3. Rotations in Three Dimensions

$O(3)$ rotations, i.e. rotations of three dimensional real vectors, have been implemented in the *Math::ThreeRotationMatrix* class in `three_rotation.hpp`. The class *Math::ThreeVector* represents three dimensional vectors, which can be passed as an input to *Math::ThreeRotationMatrix* to be rotated. The user can set the rotation matrix either by specifying three Euler angles (ϕ, θ, ψ) , or by giving an axis and an angle of rotation around that axis. The user can then read the matrix elements, or perform a rotation on a given vector. The multiplication operation has been defined for these matrices.

By default, the rotation is passive, i.e. the coordinate frame is rotated rather than the vector. The convention for Euler angles is as follows. First a counterclockwise rotation is performed around the z axis by angle ϕ , then a counterclockwise rotation around the new x axis by angle θ , and finally a counterclockwise rotation around the new z axis by angle ψ .

7.4. Wigner $3 - j$ Symbols

The main method for computing the Wigner $3 - j$ symbols is by using recursion relations, and this is how most of the numerical libraries implement the calculation. Most of the time, however, one needs to calculate a lot of these symbols at once. Numerical libraries, such as the GNU Scientific Library [40], have functions for calculating each symbol by itself. When one calls these functions many times for a range of indices, a lot of the calculation is repeated many times, because to calculate the values for higher indices these functions need to calculate all of the lower index symbols again to use recursion. We

¹Note that the *Math::RealFunction* type is the same as *Math::Function<double, double>*, i.e. it is a specific case of *Math::Function* with the variable types fixed to be real numbers.

have solved this problem in Cosmo++ by creating an interface that allows the user to first set the maximum value for the indices, after which the symbols are sent back one by one as they are being calculated. This allows for the whole calculation to be performed only once. Compared to the case when each symbol is calculated from scratch, our approach gives a huge improvement in computational time. We use this implementation to calculate the mask coupling kernel (15), for example, where all of the symbols are needed with indices up to a given maximum value.

The current version of Cosmo++ only includes the implementation for the case when all of the m indices are 0. This is done in the template class `Math::Wigner3JZeroM` in `wigner_3j.hpp`. The template parameter is a simple class that needs to include a *process* function. The symbols are then sent back to the user by calling the *process* function for an object given by the user.

7.5. Random Number Generator

Cosmo++ includes two random number generators: a Gaussian distribution generator `Math::GaussianGenerator` and a Poisson distribution generator `Math::PoissonGenerator`. Both of these classes are defined in `random.hpp`. The implementation uses the publicly available C++ Boost library [41].

7.6. Curve Fitting

Basic curve fitting functionality is included in Cosmo++ through the class `Math::Fit` in `fit.hpp`. The function to be fit to the data points is passed as a parametric function, and the number of the parameters is a template argument. Specifically, a child class of the class `Math::ParametricFunction` needs to be implemented and passed to `Math::Fit` as an input. As a useful case, we have implemented a polynomial parametric function (the parameters are the coefficients of the polynomial) in the class `Math::Polynomial` in `polynomial.hpp`.

The curve fitting is done by simply minimizing $\chi^2 = \sum_i (y_i - f(x_i))^2$ as a function of the parameters. Here (x_i, y_i) denote the data points, f denotes the function to be fit. The minimization is done using the publicly available C++ package Minuit [42].

8. Examples

We have implemented a few examples that can help the user better understand the functionality of the library. Some of these examples may be useful on their own.

8.1. CMB power spectra calculation

The file `test.cpp` includes a simple calculation of CMB power spectra. The values of the standard cosmological parameters are defined, then an instance of the `CMB` class is created with these parameters, the power spectra are calculated, and the results are written in text files. Upon compilation, this file is turned into the executable `test`.

8.2. Planck Likelihood

The Planck likelihood code [8] is publicly available and can be used as a library to be linked to other code. Since most of the current research in cosmology uses this code, we found it useful to include an interface in Cosmo++. This also serves as a useful example of implementing an instance of the abstract class `Math::LikelihoodFunction` described in Section 4, which can be directly used by the parameter space samplers. The user may choose to compile Cosmo++ without linking to the Planck likelihood code in which case the functionality described above will be absent.

The Planck likelihood interface is implemented in the `PlanckLikelihood` class in `planck_like.hpp`. Our implementation allows the user to set the cosmological parameters first, then any extra parameters that are used for modelling the foreground effects, after which different Planck likelihoods can be calculated. The user can also calculate the combination of all of the likelihoods that were chosen in the constructor through the function `calculate`. This function is used by the parameter space samplers described in Section 4.

A simple tester of this functionality is implemented in `test_planck.cpp` which is compiled into the executable `test_planck`.

8.3. Parameter Space Sampling

As a simple but a very useful case of parameter space sampling we have implemented a MultiNest sampler for the Planck likelihood code in `mn_scan_planck.cpp`. After compiling Cosmo++ this turns into the executable `mn_scan_planck` which can be used directly to calculate the posterior distributions and the confidence intervals of the standard cosmological parameters from Planck. This example can be used as a good starting point for constructing parameter space scanning codes with different likelihoods and different scanners. The example contains only about 50 lines of code, and is very straightforward to change and generalize.

9. Tests

We have performed multiple rigorous tests of all of the modules of Cosmo++. We describe some of the most important tests below.

9.1. Mathematical Tools

We have separately tested all of the mathematical tools described in Section 7. The conjugate gradient solver has been tested by solving a few linear equations with two and three variables. The three dimensional rotation matrices and the Wigner $3-j$ symbols have been tested by comparing some sample results with calculations using the Mathematica software [43]. We have tested the interpolation and curve fitting routines by choosing 7 random points, then doing a linear and cubic spline interpolation to them, as well as fitting a third degree polynomial to these points. The results are shown in Figure 1.

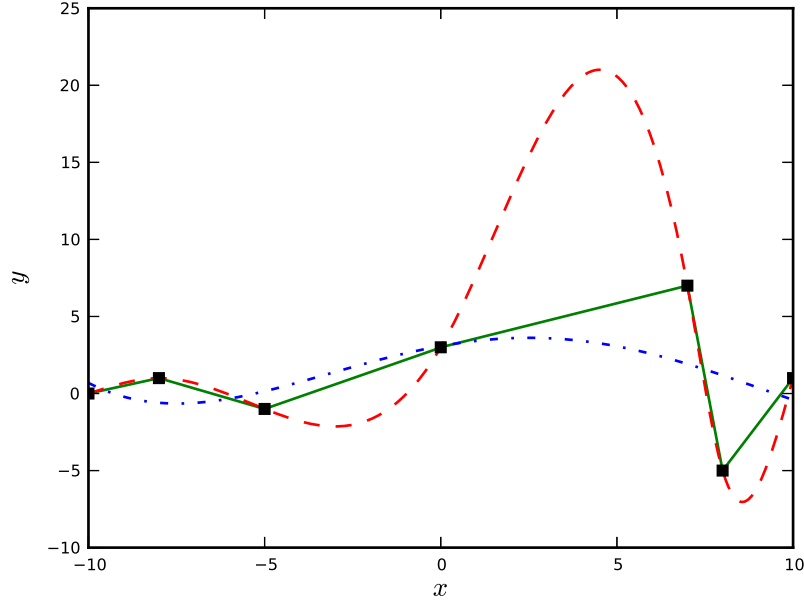


Figure 1: Testing the interpolation and curve fitting routines. The black square points have been chosen randomly, the green solid curve is obtained by linear interpolation, the red dashed curve is a cubic spline interpolation, and the blue dash-dotted curve is a cubic polynomial fit to the points.

9.2. Mask Apodization

We combine the SMICA, SEVEM, and NILC masks from Planck [44] to obtain a sample mask (this is very similar to the Planck U73 mask, which is not publicly available). We then downgrade this mask to HEALPix $N_{side} = 128$ using the *ud_grade* routine and then keep only those pixels unmasked which have a value greater than 0.5. We use this resulting mask to test our apodization routines. The original mask, as well as 7° apodized masks with cosine and Gaussian apodization are shown in Figure 2. We have chosen the low resolution and the large apodization angle for demonstration purposes; in practice these routines are used for higher resolution maps with much smaller apodization angles.

9.3. Simulations and Likelihood Calculation

To test the likelihood calculation and simulation routines in Cosmo++, we simulate 5,000 sky and noise maps, mask them, then calculate the likelihoods for the signal and noise power spectra used for simulations. The simulations are done in harmonic space, then converted into pixel space using HEALPix. The signal and noise power spectra used for our simulations are shown in Figure

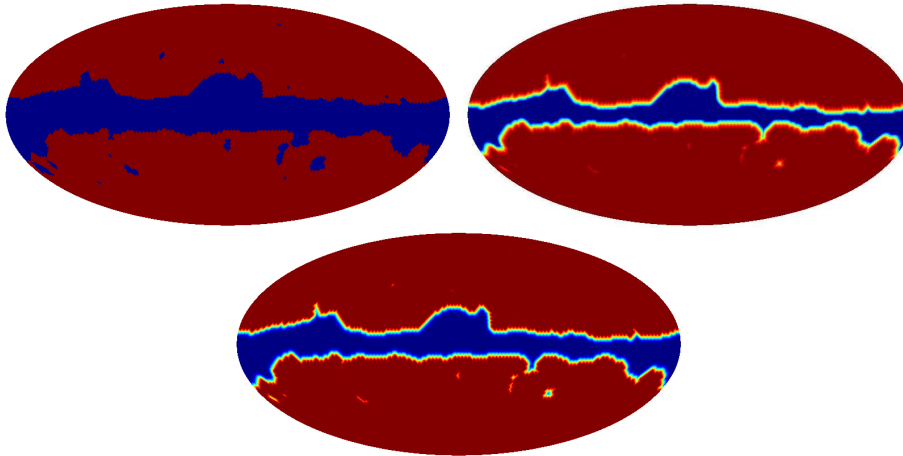


Figure 2: Original sample mask (top left), cosine apodized mask (top right), Gaussian apodized mask (bottom). The apodization angle for both cases is 7° .

3. The signal power spectrum is calculated using typical Λ CDM parameter values, the noise model is chosen to be close to the instrumental noise in Planck temperature maps [8]. The maps are signal dominated up to $l \approx 1750$. The simulations have HEALPix $N_{side} = 2048$.

We divide the likelihood calculation into two regimes: low- l ($l = 2 \rightarrow 30$) and high- l ($l = 31 \rightarrow 2000$). We use the combined Planck mask as described in Section 9.2 at the original resolution of $N_{side} = 2048$ for the high- l calculation. However, we apodize the mask with a $30'$ cosine function. We use the *Master* class to first calculate the best-fit power spectra, then we pass the results to the *LikelihoodHigh* class for calculating the likelihood values.

At low- l we use the pixel space likelihood calculation class. The maps are smoothed with a 10° Gaussian beam and downgraded to $N_{side} = 16$. The mask is first smoothed with a 10° Gaussian beam, then downgraded to $N_{side} = 16$ with the *ud_grade* routine in HEALPix, then the pixels with value greater than 0.8 are kept unmasked, the rest is masked. This leaves 2,426 pixels. Since the noise level is negligible at this low resolution, we add $1 \mu\text{K}$ uniform white noise to the maps to regularize the covariance matrix inversion (see Section 3).

The resulting χ^2 distributions for both cases, along with the expected distributions, are shown in Figure 4. For the low- l case the expected distribution has 2,426 degrees of freedom (the number of unmasked pixels). For the high- l case the expected distribution has 1,970 degrees of freedom (the number of l values included). The agreement between the resulting distribution and the expected distribution is excellent for both cases.

9.4. Parameter Constraints from Planck

As a final test, we run the MultiNest sampler with different likelihood functions to calculate the posterior distributions and the resulting confidence inter-

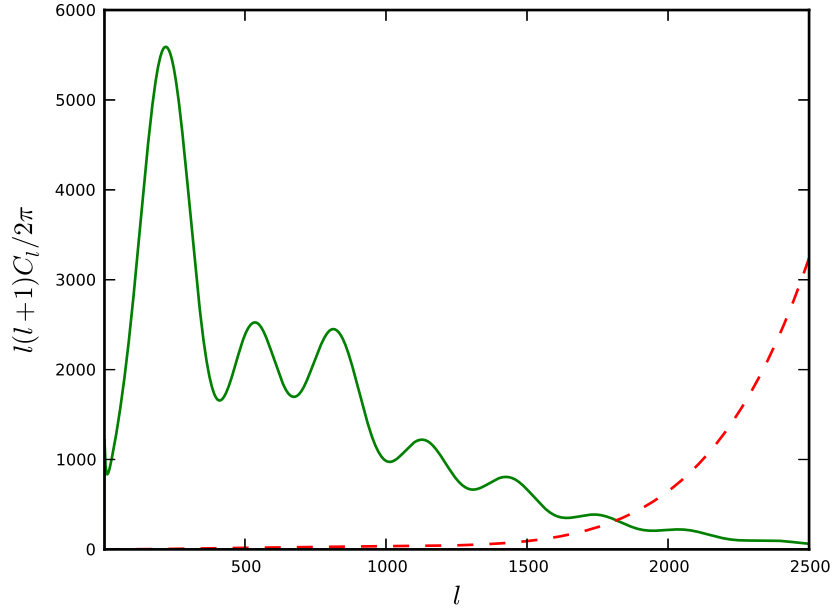


Figure 3: The signal (green solid curve) and noise (red dashed curve) power spectra for the simulations. The units are μK^2 .

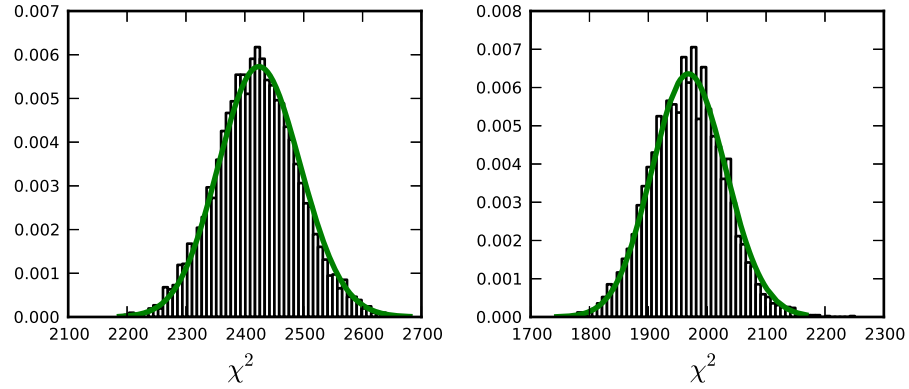


Figure 4: The χ^2 distribution from 5,000 simulations (black histogram) compared to the expected distribution (green solid curve). Low- l pixel space likelihood calculation is on the left, high- l harmonic space likelihood calculation is on the right.

Parameter	Planck	Cosmo++
h	0.679 ± 0.015	0.684 ± 0.014
$\Omega_b h^2$	0.02217 ± 0.00033	0.02219 ± 0.00032
$\Omega_c h^2$	0.1186 ± 0.0031	0.1185 ± 0.0030
τ	0.089 ± 0.032	0.090 ± 0.030
n_s	0.9635 ± 0.0094	0.9625 ± 0.0090
$\ln(10^{10} A_s)$	3.085 ± 0.057	3.085 ± 0.054

Table 1: Parameter constraints by Planck [45], as well as our results from Cosmo++ using the Planck likelihood code together with the MultiNest sampler.

Parameter	Pixel Space	Gibbs
h	0.688 ± 0.009	0.694 ± 0.009
$\Omega_b h^2$	0.02218 ± 0.00021	0.02226 ± 0.00021
$\Omega_c h^2$	0.1174 ± 0.0019	0.1162 ± 0.0019
τ	0.086 ± 0.010	0.085 ± 0.010
n_s	0.9558 ± 0.0057	0.9602 ± 0.0056
$\ln(10^{10} A_s)$	3.073 ± 0.020	3.068 ± 0.019

Table 2: Parameter constraints from the SMICA map using the pixel space likelihood calculation for low- l compared to the Gibbs sampler.

vals for the standard Λ CDM parameters. We first use the Planck likelihood code together with the MultiNest sampler to constrain the parameters. The results can be directly compared with the published results by the Planck collaboration [45]. We use the Planck likelihood together with lensing. Our results, together with the results released by Planck, are given in Table 1. The agreement is excellent. There are very small differences which may arise mainly because we used h instead of θ_{MC} (the ratio of the angular diameter distance to the last scattering surface sound horizon) for sampling. Other small differences could arise because of using a different parameter space sampler.

Next we use our own likelihood codes (see Section 3) applied to the SMICA map by Planck. We expect to get similar parameter constraints as from the Planck likelihood code. We use the combined mask as described in the previous section. To test both of the low- l likelihood codes, we do the sampling with two different combinations of our likelihood classes. Firstly, we use our pixel

space likelihood code for l values between 2 and 30 applied to the SMICA map smoothed to 10° and downgraded to $N_{side} = 16$ together with the high- l likelihood code for $l = 31 \rightarrow 1750$. Our second calculation uses the CMB Gibbs sampler for $l = 2 \rightarrow 50$ applied to the SMICA map smoothed to 5° and downgraded to $N_{side} = 32$ together with the high- l likelihood code for $l = 51 \rightarrow 1750$. Since no polarization or lensing data is included in this case, we put an informative Gaussian prior on τ of $\tau = 0.0851 \pm 0.014$, following the corresponding analysis by Planck [44]. We model the foreground contamination effects by two parameters: A_{ps} (the amplitude of the Poisson component) and A_{cl} (the amplitude of the clustered component), in the exact same way as done in [44]. We have used the MultiNest sampler for scanning the parameter space. The results are summarized in Table 2. We can see that there is a very good agreement between the results from the two different likelihood codes used for low- l . Moreover, the parameter constraints agree very well with those from the full Planck likelihood code. The main difference is that we get smaller error bars for the SMICA map, and this can happen because of a few reasons. First of all, we use a tight Gaussian prior on τ for the SMICA analysis, while for the Planck likelihood analysis we used an uninformative uniform prior. Secondly, the foreground contamination is assumed to be mainly cleaned in SMICA. The sampling uses only two parameters to model the foreground contamination, compared to the 14 foreground parameters used in the Planck likelihood code. Thirdly, we used the publicly available noise map for SMICA to estimate the noise power spectrum. This may have slightly underestimated the noise power spectrum at small scales because of the bias effects described in [44]. Nonetheless, the constraints for all of the parameters (except for τ) from SMICA and the full likelihood code are within the error bars of each other.

To compare the two parameter space samplers, we have repeated the scans for the SMICA map with our Metropolis-Hastings sampler. We used standard Gaussian proposal distributions with typical widths. The resulting posterior distributions are almost indistinguishable from the MultiNest results discussed above. In terms of computational time, however, MultiNest outperforms the Metropolis-Hastings sampler unless the proposal distributions and their widths are chosen carefully.

10. Summary

We have described a new numerical library for cosmology written entirely in C++. The object-oriented design has made it possible to clearly separate different parts of the library into different classes, each one of which can be used on its own. Multiple rigorous tests have been performed to check the functionality of the library. Although the code is fully documented, we have included a few examples to help the user get started.

The library is complete in the sense that it can be applied directly to publicly available data to calculate the posterior distributions and the confidence intervals for cosmological parameters. It also includes full functionality for performing CMB sky simulations, as well as numerous additional tools that are

frequently used in cosmological research. However, as discussed throughout the paper, there are multiple useful features that can be added to the library. We are planning to add a few new features to the future releases of the library. The input of the scientific community will be crucial in determining the most important new features that we need to add to Cosmo++.

I thank Layne Price and Richard Easther for useful discussions and comments on the manuscript. I also thank Amit Yadav for helpful discussions on the implementation of certain parts of the code.

The author wishes to acknowledge the contribution of the NeSI high performance computing facilities and the staff at the Centre for eResearch at the University of Auckland. New Zealand’s national facilities are provided by the New Zealand eScience Infrastructure (NeSI) and funded jointly by NeSI’s collaborator institutions and through the Ministry of Business, Innovation and Employment’s Infrastructure programme [46].

Appendix A. Notation and Units

Appendix A.1. Cosmological Parameters

We denote the Hubble parameter by H ; it has units of km/s/Mpc. The unitless form h is defined by $H = 100 h$ km/s/Mpc.

Unitless density parameters are defined by

$$\Omega_i = \rho_i / \rho_{\text{cr}} \quad (\text{A.1})$$

where ρ_i denotes the given type of density, ρ_{cr} is the critical density, i.e. the density of the universe with zero spatial curvature

$$\rho_{\text{cr}} = \frac{3H^2}{8\pi G} \quad (\text{A.2})$$

where G denotes the gravitational constant. Ω_b denotes the baryon density, Ω_c denotes the density of cold dark matter, $\Omega_m = \Omega_b + \Omega_c$ denotes the total matter density, Ω_Λ denotes the dark energy density, Ω_γ denotes the photon density, Ω_ν denotes the density of neutrinos, $\Omega_r = \Omega_\gamma + \Omega_\nu$ denotes the total radiation density, Ω_K denotes the curvature density.

We denote by N_{eff} the number of effective degrees of freedom for relativistic particles (neutrinos for example). In the standard Λ CDM model $N_{\text{eff}} = 3.046$ [47].

Non cold dark matter particles, such as massive neutrinos, are described by their number N_{NCDM} , their mass $m_{\text{NCDM},i}$ in eV, and the ratio of their temperature to the photon temperature $T_{\text{NCDM},i}$.

The reionization optical depth τ is used to describe reionization. Y_{He} denotes the Helium mass fraction.

Appendix A.2. Cosmic Microwave Background Radiation Maps

The Cosmic Microwave Background radiation temperature T_{CMB} is given in units of K. The default value is $T_{\text{CMB}} = 2.726$ K. The CMB anisotropy maps have units of μK by default.

We denote the CMB temperature anisotropies in direction $\hat{\mathbf{n}}$ by $T(\hat{\mathbf{n}})$, and the polarization Q and U modes by $Q(\hat{\mathbf{n}})$ and $U(\hat{\mathbf{n}})$, respectively. These maps can be decomposed into spherical harmonics

$$T(\hat{\mathbf{n}}) = \sum_{lm} T_{lm} Y_{lm}(\hat{\mathbf{n}}), \quad (\text{A.3})$$

$$Q(\hat{\mathbf{n}}) \pm iU(\hat{\mathbf{n}}) = \sum_{lm} {}_{\mp 2}a_{lm} {}_{\mp 2}Y_{lm}(\hat{\mathbf{n}}) \quad (\text{A.4})$$

where ${}_s Y_{lm}$ are the spin-weighted spherical harmonics. The polarization coefficients are further decomposed into real and imaginary parts (E and B modes) [24]

$${}_{\pm 2}a_{lm} = E_{lm} \pm iB_{lm}. \quad (\text{A.5})$$

We use the HEALPix format [1] to represent the anisotropy maps in pixel space. The value of the map \mathcal{X} (T , Q , or U) in pixel i is denoted by \mathcal{X}_i . This is related to the underlying map $\mathcal{X}(\hat{\mathbf{n}})$ by

$$\mathcal{X}_i = \int d\hat{\mathbf{n}} \mathcal{X}(\hat{\mathbf{n}}) B_i(\hat{\mathbf{n}}) \quad (\text{A.6})$$

where B_i is the beam function at pixel i , and is specific to the experiment. By default, we include the HEALPix pixel window functions [1] in the beam function.

Usually the beam functions have the same shape for every pixel and are axially symmetric around the center of the pixel. In this case the beam function can be decomposed into spherical harmonics as follows

$$B_i(\hat{\mathbf{n}}) = \sum_{lm} B_l Y_{lm}(\hat{\mathbf{n}}_i) Y_{lm}^*(\hat{\mathbf{n}}) \quad (\text{A.7})$$

where $\hat{\mathbf{n}}_i$ denotes the direction of pixel i .

Appendix A.3. Covariance Matrices

We denote the two-point correlation function in pixel space by

$$C_{ij}^{\mathcal{X}\mathcal{Y}} = \langle \mathcal{X}_i \mathcal{Y}_j \rangle, \quad (\text{A.8})$$

and in harmonic space by

$$M_{lm'l'm'}^{\mathcal{X}\mathcal{Y}} = \langle \mathcal{X}_{lm} \mathcal{Y}_{l'm'}^* \rangle. \quad (\text{A.9})$$

In harmonic space \mathcal{X} and \mathcal{Y} denote T , E , and B .

When statistical rotational invariance is satisfied, the covariance matrices are diagonal in harmonic space

$$M_{lm'l'm'}^{\mathcal{X}\mathcal{Y}} = \delta_{ll'}\delta_{mm'}C_l^{\mathcal{X}\mathcal{Y}}, \quad (\text{A.10})$$

and $C_l^{\mathcal{X}\mathcal{Y}}$ denotes the conventional power spectrum in harmonic space.

The covariance matrices have units of μK^2 , by default. When there is no ambiguity, we sometimes omit the superscripts $\mathcal{X}\mathcal{Y}$. By default, we do not include any extra factors in C_l , such as $l(l+1)/2\pi$, as is sometimes done in the literature.

Appendix A.4. Primordial Perturbations

We use the gauge invariant curvature perturbations on uniform density hypersurfaces $\zeta(\mathbf{x})$ to describe the primordial scalar perturbations [48]. The transformation to Fourier space is given by

$$\zeta(\mathbf{x}) = \int \frac{d^3k}{(2\pi)^3} e^{i\mathbf{k}\cdot\mathbf{x}} \zeta(\mathbf{k}). \quad (\text{A.11})$$

For Gaussian perturbations, all of the information is contained in the two-point function. In case of statistically homogeneous fluctuations, the two-point function takes the form

$$\langle \zeta(\mathbf{k})\zeta^*(\mathbf{k}') \rangle = (2\pi)^3 \delta^3(\mathbf{k} - \mathbf{k}') P_\zeta(k), \quad (\text{A.12})$$

and $P_\zeta(k)$ is called the power spectrum.

We define the dimensionless power spectrum in Fourier space

$$\Delta_\zeta^2(k) \equiv \frac{k^3}{2\pi^2} P_\zeta(k). \quad (\text{A.13})$$

Similar definitions hold for the tensor perturbations h_{ij} [48]. In what follows, the term ‘‘primordial power spectrum’’ will refer to the dimensionless case, unless stated otherwise.

Standard inflationary theory predicts a nearly scale invariant primordial power spectrum [48]. The canonical parametrization of the power spectra is as follows

$$\Delta_\zeta^2(k) = A_s \left(\frac{k}{k_*} \right)^{n_s - 1 + \frac{1}{2}\alpha_s \ln(k/k_*)}, \quad (\text{A.14})$$

$$\Delta_h^2(k) = A_t \left(\frac{k}{k_*} \right)^{n_t + \frac{1}{2}\alpha_t \ln(k/k_*)} \quad (\text{A.15})$$

where A_s and A_t are the scalar and tensor amplitudes, respectively; n_s and n_t are the spectral indices; $\alpha_s = dn_s/d\ln k$ and $\alpha_t = dn_t/d\ln k$ are the runnings of the spectral indices. k_* denotes a chosen pivot scale. The units of k are Mpc^{-1} by default.

The tensor-to-scalar ratio is defined as

$$r \equiv \frac{\Delta_h^2(k_*)}{\Delta_\zeta^2(k_*)}. \quad (\text{A.16})$$

References

- [1] K. M. Gorski, E. Hivon, A. J. Banday, B. D. Wandelt, F. K. Hansen, M. Reinecke, M. Bartelmann, HEALPix: a framework for high-resolution discretization and fast analysis of data distributed on the sphere, *The Astrophysical Journal* 622 (2) (2005) 759.
- [2] A. Lewis, A. Challinor, A. Lasenby, Efficient computation of cosmic microwave background anisotropies in closed Friedmann-Robertson-Walker models, *The Astrophysical Journal* 538 (2) (2000) 473.
- [3] J. Lesgourgues, The Cosmic Linear Anisotropy Solving System (CLASS) I: Overview, arXiv:1104.2932.
- [4] D. Blas, J. Lesgourgues, T. Tram, The Cosmic Linear Anisotropy Solving System (CLASS). Part II: Approximation schemes, *Journal of Cosmology and Astroparticle Physics* 2011 (07) (2011) 034.
- [5] N. Jarosik, C. L. Bennett, J. Dunkley, B. Gold, M. R. Greason, M. Halpern, R. S. Hill, G. Hinshaw, A. Kogut, E. Komatsu, Seven-year Wilkinson Microwave Anisotropy Probe (WMAP) observations: sky maps, systematic errors, and basic results, *ApJS* 192 (2) (2011) 14.
- [6] D. Larson, J. Dunkley, G. Hinshaw, E. Komatsu, M. R. Nolta, C. L. Bennett, B. Gold, M. Halpern, R. S. Hill, N. Jarosik, Seven-year Wilkinson Microwave Anisotropy Probe (WMAP) observations: power spectra and WMAP-derived parameters, *ApJS* 192 (2) (2011) 16.
- [7] E. Komatsu, K. M. Smith, J. Dunkley, C. L. Bennett, B. Gold, G. Hinshaw, N. Jarosik, D. Larson, M. R. Nolta, L. Page, Seven-year Wilkinson microwave anisotropy probe (WMAP) observations: cosmological interpretation, *ApJS* 192 (2) (2011) 18.
- [8] P. Collaboration, Planck 2013 results. XV. CMB power spectra and likelihood, arXiv:1303.5075.
- [9] A. Lewis, S. Bridle, Cosmological parameters from CMB and other data: A Monte Carlo approach, *Physical Review D* 66 (10) (2002) 103511.
- [10] P. Collaboration, Planck 2013 results. XXVI. Background geometry and topology of the Universe, arXiv:1303.5086.
- [11] G. Aslanyan, A. V. Manohar, A. P. S. Yadav, The topology and size of the universe from CMB temperature and polarization data, *Journal of Cosmology and Astroparticle Physics* 08 (0) (2013) 009.
- [12] J. Kim, E. Komatsu, Limits on anisotropic inflation from the Planck data, *Physical Review D* 88 (1) (2013) 101301.

- [13] N. E. Groeneboom, L. Ackerman, I. K. Wehus, H. K. Eriksen, Bayesian Analysis of an Anisotropic Universe Model: Systematics and Polarization, *The Astrophysical Journal* 722 (1) (2010) 452–459.
- [14] P. Collaboration, Planck 2013 results. XXIII. Isotropy and Statistics of the CMB, arXiv:1303.5083.
- [15] W. R. Gilks, S. Richardson, D. J. Spiegelhalter, *Markov Chain Monte Carlo In Practice*, Chapman and Hall, 1996.
- [16] F. Feroz, M. P. Hobson, M. Bridges, MultiNest: an efficient and robust Bayesian inference tool for cosmology and particle physics, *Monthly Notices of the Royal Astronomical Society* 398 (4) (2009) 1601–1614.
- [17] F. Feroz, M. P. Hobson, E. Cameron, A. N. Pettitt, Importance Nested Sampling and the MultiNest Algorithm, arXiv:1306.2144.
- [18] F. Feroz, M. P. Hobson, Multimodal nested sampling: an efficient and robust alternative to Markov Chain Monte Carlo methods for astronomical data analyses, *Monthly Notices of the Royal Astronomical Society* 384 (2) (2008) 449–463.
- [19] [link].
URL www.doxygen.org
- [20] M. Bridges, F. Feroz, M. P. Hobson, A. N. Lasenby, Bayesian optimal reconstruction of the primordial power spectrum, *Monthly Notices of the Royal Astronomical Society* 400 (2) (2009) 1075–1084.
- [21] L. Verde, H. Peiris, On minimally parametric primordial power spectrum reconstruction and the evidence for a red tilt, *Journal of Cosmology and Astroparticle Physics* 07 (0) (2008) 009.
- [22] H. V. Peiris, L. Verde, The shape of the primordial power spectrum: A last stand before Planck data, *Physical Review D* 81 (2) (2010) 21302.
- [23] G. Efstathiou, Myths and truths concerning estimation of power spectra: the case for a hybrid estimator, *Monthly Notices of the Royal Astronomical Society* 349 (2) (2004) 603–626.
- [24] L. Page, G. Hinshaw, E. Komatsu, M. R. Nolta, D. N. Spergel, C. L. Bennett, C. Barnes, R. Bean, O. Doré, J. Dunkley, M. Halpern, R. S. Hill, N. Jarosik, A. Kogut, M. Limon, S. S. Meyer, N. Odegard, H. V. Peiris, G. S. Tucker, L. Verde, J. L. Weiland, E. Wollack, E. L. Wright, Three-Year Wilkinson Microwave Anisotropy Probe (WMAP) Observations: Polarization Analysis, *ApJS* 170 (2) (2007) 335–376.
- [25] G. Hinshaw, M. R. Nolta, C. L. Bennett, R. Bean, O. Doré, M. R. Greason, M. Halpern, R. S. Hill, N. Jarosik, A. Kogut, E. Komatsu, M. Limon, N. Odegard, S. S. Meyer, L. Page, H. V. Peiris, D. N. Spergel, G. S. Tucker,

- L. Verde, J. L. Weiland, E. Wollack, E. L. Wright, Three-Year Wilkinson Microwave Anisotropy Probe (WMAP) Observations: Temperature Analysis, *ApJS* 170 (2) (2007) 288–334.
- [26] G. Hinshaw, D. N. Spergel, L. Verde, R. S. Hill, S. S. Meyer, C. Barnes, C. L. Bennett, M. Halpern, N. Jarosik, A. Kogut, E. Komatsu, M. Limon, L. Page, G. S. Tucker, J. L. Weiland, E. Wollack, E. L. Wright, First-Year Wilkinson Microwave Anisotropy Probe (WMAP) Observations: The Angular Power Spectrum, *ApJS* 148 (1) (2003) 135–159.
- [27] E. Hivon, K. M. Gorski, C. B. Netterfield, B. P. Crill, S. Prunet, F. Hansen, MASTER of the Cosmic Microwave Background Anisotropy Power Spectrum: A Fast Method for Statistical Analysis of Large and Complex Cosmic Microwave Background Data Sets, *The Astrophysical Journal* 567 (1) (2002) 2–17.
- [28] M. Tegmark, How to measure CMB power spectra without losing information, *Physical Review D* 55 (1) (1997) 5895–5907.
- [29] G. Rocha, C. R. Contaldi, J. R. Bond, K. M. Górski, Application of XFASTER power spectrum and likelihood estimator to Planck, *Monthly Notices of the Royal Astronomical Society* 414 (2) (2011) 823–846.
- [30] L. Verde, H. V. Peiris, D. N. Spergel, M. R. Nolta, C. L. Bennett, M. Halpern, G. Hinshaw, N. Jarosik, A. Kogut, M. Limon, S. S. Meyer, L. Page, G. S. Tucker, E. Wollack, E. L. Wright, First-Year Wilkinson Microwave Anisotropy Probe (WMAP) Observations: Parameter Estimation Methodology, *ApJS* 148 (1) (2003) 195–211.
- [31] H. K. Eriksen, I. J. O’Dwyer, J. B. Jewell, B. D. Wandelt, D. L. Larson, K. M. Górski, S. Levin, A. J. Banday, P. B. Lilje, Power Spectrum Estimation from High-Resolution Maps by Gibbs Sampling, *ApJS* 155 (2) (2004) 227–241.
- [32] N. E. Groeneboom, A self-contained guide to the CMB Gibbs sampler, [arXiv:0905.3823](https://arxiv.org/abs/0905.3823).
- [33] H. K. Eriksen, J. B. Jewell, C. Dickinson, A. J. Banday, K. M. Górski, C. R. Lawrence, Joint Bayesian Component Separation and CMB Power Spectrum Estimation, *The Astrophysical Journal* 676 (1) (2008) 10–32.
- [34] J. R. Shewchuk, An introduction to the conjugate gradient method without the agonizing pain.
- [35] Ø. Rudjord, N. E. Groeneboom, H. K. Eriksen, G. Huey, K. M. Górski, J. B. Jewell, Cosmic Microwave Background Likelihood Approximation by a Gaussianized Blackwell-Rao Estimator, *The Astrophysical Journal* 692 (2) (2009) 1669–1677.

- [36] R. Allison, J. Dunkley, Comparison of sampling techniques for Bayesian parameter estimation, arXiv:1308.2675.
- [37] P. Scott, Pippi — Painless parsing, post-processing and plotting of posterior and likelihood samples, The European Physical Journal Plus 127 (2012) 138.
- [38] A. de Oliveira-Costa, M. Tegmark, M. Zaldarriaga, A. Hamilton, Significance of the largest scale CMB fluctuations in WMAP, Physical Review D 69 (6) (2004) 63516.
- [39] G. Aslanyan, R. Easter, Large Scale Anomalies in the Microwave Background: Causation and Correlation, arXiv:1308.6593.
- [40] [link].
URL <http://www.gnu.org/software/gsl/>
- [41] [link].
URL <http://www.boost.org>
- [42] [link].
URL <http://seal.web.cern.ch/seal/work-packages/mathlibs/minuit>
- [43] [link].
URL <http://www.wolfram.com/mathematica/>
- [44] P. Collaboration, Planck 2013 results. XII. Component separation, arXiv:1303.5072.
- [45] P. Collaboration, Planck 2013 results. I. Overview of products and scientific results, arXiv:1303.5062.
- [46] [link].
URL <http://www.nesi.org.nz>
- [47] S. Dodelson, Modern Cosmology, Academic Press, 2003.
- [48] D. Baumann, TASI lectures on inflation, arXiv:0907.5424.